



Faller, K. M.E. et al. (2016) The Chihuahua dog: A new animal model for neuronal ceroid lipofuscinosis CLN7 disease? *Journal of Neuroscience Research*, 94(4), pp. 339-347. (doi:[10.1002/jnr.23710](https://doi.org/10.1002/jnr.23710))

This is the author's final accepted version.

There may be differences between this version and the published version. You are advised to consult the publisher's version if you wish to cite from it.

<http://eprints.gla.ac.uk/117146/>

Deposited on: 21 June 2016

1 **The Chihuahua dog, a new animal model for Neuronal Ceroid Lipofuscinosis**
2 **CLN7 disease?**

3

4 **Kiterie M. E. Faller¹, Jose Bras², Samuel J. Sharpe¹, Glenn W. Anderson³, Lee**
5 **Darwent², Celia Kun-Rodrigues², Joseph Alroy⁴, Jacques Penderis⁵, Sara E.**
6 **Mole⁶, Rodrigo Gutierrez-Quintana^{1*}, Rita J. Guerreiro^{2*}**

7

8 *** Joint senior authorship**

- 9 *1. School of Veterinary Medicine, College of Medical, Veterinary and Life Sciences,*
10 *University of Glasgow, Bearsden Road, Glasgow, G61 1QH, UK*
11 *2. Department of Molecular Neuroscience, Institute of Neurology, University College*
12 *London, Queen Square, London, WC1N 3BG, UK*
13 *3. Department of Histopathology, Great Ormond Street Hospital, London, WC1N*
14 *3JH, UK*
15 *4. Department of Pathology, Tufts University School of Medicine and Tufts-New*
16 *England Medical Center, Boston, Massachusetts 02111, USA*
17 *5. VetExtra Neurology, Craig Leith Road, Broadleys, Stirling, FK7 7LE, UK*
18 *6. MRC laboratory for Molecular Cell Biology, UCL institute of Child Health, and*
19 *Department of Genetics, Evolution and Environment, University College London,*
20 *Gower Street, London, WC1E 6BT, UK*

21

22 Running head: The Chihuahua dog, a model for CLN7 disease

23

24 Associate editor: Dr Aurora Pujol Onofre

25

26 Keywords: MFSD8, lysosomal storage disorder, neurodegeneration

27

28 Corresponding author: Tel.: +44 141 3305848; fax: +44 141 3303663; *Email address:*
29 *Rodrigo.GutierrezQuintana@glasgow.ac.uk (Rodrigo Gutierrez-Quintana)*

30

31 Support information: This study was funded by a grant from the University of
32 Glasgow Small Animal Hospital Fund. J.B. and R.J.G. are supported by fellowships
33 from the Alzheimer's Society.

34

35

36 An abstract of part of this work has been submitted for presentation at the Annual

37 Congress of the European College of Veterinary Neurology.

38

39 ABSTRACT

40 Neuronal ceroid lipofuscinoses (NCL) are a group of incurable lysosomal storage
41 disorders characterized by neurodegeneration and accumulation of lipopigments
42 mainly within the neurons. We studied two littermate Chihuahua dogs presenting with
43 progressive signs of blindness, ataxia, pacing and cognitive impairment from the age
44 of one year old. Due to worsening of clinical signs, both dogs were euthanized at
45 around two years of age. Post-mortem examination revealed marked accumulation of
46 autofluorescent intracellular inclusions within the brain, characteristic of NCL. Whole
47 genome sequencing was performed on one of the affected dogs. Following sequence
48 alignment and variant calling against the canine reference genome, variants were
49 identified in the coding region or splicing regions of four previously known NCL
50 genes (*CLN6*, *ARSG*, *CLN2=TPPI* and *CLN7=MFSD8*). Subsequent segregation
51 analysis within the family (two affected dogs, both parents and three relatives)
52 identified *MFSD8*:p.Phe282Leufs13* as the causal mutation, which had previously
53 been identified in one Chinese crested dog with no available ancestries. Due to the
54 similarities of the clinical signs and histopathological changes with the human form of
55 the disease, we propose that the Chihuahua dog could be a good animal model of
56 CLN7 disease.

57

58

59 SIGNIFICANCE STATEMENT

60 NCL are a group of incurable lysosomal storage disorders unified by similar
61 histopathological changes. Although mutations in 13 genes coding for functionally
62 distinct proteins have been identified, the pathophysiology of these diseases is still
63 poorly understood. Naturally occurring large animal models have had an invaluable
64 contribution to better understand the pathophysiology and therapeutic options of some
65 forms of NCL. CLN7 is a poorly characterized form, and this could be due to a lack
66 of animal models that closely reproduce the human phenotype. We identified
67 Chihuahua dogs with a genetic mutation causing CLN7 disease, which could
68 represent an excellent animal model.

69

70 INTRODUCTION

71 Neuronal Ceroid Lipofuscinoses (NCL) are a heterogeneous group of inherited
72 lysosomal storage disorders characterized by neurodegeneration and accumulation of
73 autofluorescent lipopigments mainly in neurons. In human patients, they represent the
74 most prevalent hereditary neurovisceral storage disorder with an incidence of 1.3 to 7
75 for every 100,000 live births, depending on the country (Mole and Williams, 2001
76 [Updated 2013]). Symptoms usually include blindness, motor and cognitive decline,
77 seizures and premature death. The disease was originally classified on the basis of age
78 of onset and clinical signs into congenital, infantile, late-infantile, juvenile and adult
79 forms, with many possible variants (Mole and Williams, 2001 [Updated 2013];
80 Shacka, 2012). More than 400 different mutations in thirteen genes have been
81 identified in human patients, and three genes have recently been suggested as –
82 unproven – candidate genes (Di Fruscio et al., 2015). Despite coding for functionally
83 distinct proteins – some soluble and some transmembrane proteins – mutations of
84 these genes all induce accumulation of autofluorescence storage material (Shacka,
85 2012). Mutations in different genes can result in similar phenotypes, whereas different
86 mutations in the same gene can lead to a very different disease course. This rendered
87 the original classification based on age of onset of limited value. The current
88 characterization of NCL forms is now based on the causative mutation (Mole and
89 Williams, 2001 [Updated 2013]).

90

91 Numerous animal models of NCLs have been described and have been invaluable in
92 contributing to the current understanding of this devastating condition. However,
93 despite extensive research, the disease mechanisms are still not fully understood and
94 animal models provide the opportunity to further understand the pathophysiology and

95 assess new therapeutic strategies for each different form. In veterinary medicine, NCL
96 has been described in various species including the sheep, cow, goat, horse, ferret, cat
97 and dog (Jolly and Palmer, 1995; Anderson et al., 2013). In dogs, the causative
98 mutation has been found in many breeds, including the American Bulldog (*CLN10*)
99 (Awano et al., 2006), Border Collie (*CLN5*) (Melville et al., 2005), English Setter
100 (*CLN8*) (Katz et al., 2005a), Dachshund (*CLN1* and *CLN2*) (Awano et al., 2006;
101 Sanders et al., 2010), Tibetan Terrier (*ATP13A2 = CLN12*) (Farias et al., 2011;
102 Wohlke et al., 2011), Australian Shepherd (*CLN6*) (Katz et al., 2011), Golden
103 Retriever (*CLN5*) (Gilliam et al., 2015), Australian Shepherd mix (*CLN8*) (Guo et al.,
104 2014) and more recently strongly suspected in a single Chinese Crested dog (*MFSD8*
105 = *CLN7*) (Guo et al., 2015). Mutation in *ARSG* (*Arylsulfatase G*) has also been
106 identified in the American Staffordshire Bull Terrier suffering from a lysosomal
107 storage disorder initially classified as NCL (Abitbol et al., 2010); however, more
108 recent reports suggest that *ARSG*-deficiency should be referred as a
109 mucopolysaccharidosis (more precisely MPS IIIE) (Kowalewski et al., 2012;
110 Kowalewski et al., 2015). Multiple sporadic reports of Chihuahua dogs affected by
111 NCL exist (Rac and Giesecke, 1975; Kuwamura et al., 2003; Nakamoto et al., 2011),
112 but, to date, the causative mutation has not been identified.

113 We present here a family of Chihuahua dogs with a progressive neurological disease
114 confirmed to be a form of NCL after histopathologic and ultrastructural examinations.
115 After generating a whole genome sequence using DNA from one of the affected dogs,
116 a mutation in *MFSD8* (*CLN7*) gene was identified and this was confirmed by
117 segregation analysis in the related dogs. The Chihuahua dog could represent a new
118 animal model for *CLN7* disease.

119

120 MATERIAL AND METHODS

121 1. Patient cohort – Clinical investigations

122 Two littermate Chihuahua dogs (one male and one female) were presented to the
123 Small Animal Hospital, University of Glasgow, for investigation of progressive
124 neurological signs. Following clinical examination and routine complete blood count
125 and biochemistry, they underwent magnetic resonance imaging (MRI) of the brain
126 under general anesthesia. MR images were acquired using a 1.5 T (64 MHz) system
127 (Magnetom Essenza, Siemens, Camberley, UK). T2-weighted, Fluid-attenuated
128 inversion recovery, T2*-weighted, and T1-weighted images prior and after contrast
129 were acquired in sagittal, transverse and dorsal planes. Routine cerebrospinal fluid
130 analysis including total nucleated cell count, cytology and protein measurement was
131 performed in the two affected cases and urinary organic acid screening by mass
132 spectrometry was performed in the male dog.

133

134 2. Histopathology and electron microscopy

135 The male dog was euthanized at 1 year 11 months of age and underwent a full post-
136 mortem examination. Representative samples from the cerebrum and cerebellum were
137 fixed in 2.5 % glutaraldehyde for electron microscopy (EM) analysis and other
138 samples from the cerebrum and cerebellum were embedded in Tissue-Tek O.C.T
139 (Sakura) and snapped frozen in isopentane chilled in liquid nitrogen before being
140 stored at -80 °C for fluorescence microscopy. The rest of the brain, the eyes, and
141 samples from skin, liver, kidney, adrenal, spleen, heart, duodenum and pancreas were
142 fixed in 10 % buffered formalin. Slices of the formalin-fixed brain were then
143 embedded in paraffin, before staining with hematoxilin and eosin (H&E), PAS, Sudan
144 blue and Luxol fast blue. Samples for fluorescence microscopy were analysed as

145 previously described (Katz et al., 2005b). Immunostaining was performed using
146 antibodies directed against glial fibrillary acid protein (GFAP) and lysosomal-
147 associated membrane protein 1 (LAMP-1) (see Table I for details of antibodies used).

148

149 3. Family analysis – Ethical statement

150 The breeder of the affected dogs was contacted and agreed to provide DNA samples
151 in the form of cheek swabs from the parents of the dogs and from related family
152 members (Fig. 1). EDTA blood samples were available from the two affected dogs.

153 Approval from the local ethical committee (University of Glasgow, School of
154 Veterinary Medicine) was granted (Form Ref. 12a/14) for this study.

155

156 4. Molecular analysis

157 DNA was extracted from the blood of the two affected animals using a DNeasy Blood
158 and Tissue kit (Qiagen, Crawley, UK) and from the cheek swabs using a Gentra
159 Puregene Buccal Cell Kit (Qiagen, Crawley, UK).

160 Whole-genome sequencing was performed on the affected female dog using
161 Illumina's TruSeq PCR free protocol according to the manufacturer's instructions
162 combined with Illumina's Hiseq2000 on paired-end 100bp reads. Sequence alignment
163 and variant calling were performed against the dog genome reference CanFam3.1
164 using bwa (Li and Durbin, 2009) and the Genome Analysis Toolkit respectively
165 (McKenna et al., 2010; DePristo et al., 2011), largely following the Best Practices v3,
166 with hard filters for variant recalibration. In short, this consisted of duplicate read
167 marking, realignment around indels, base quality score recalibration, variant
168 identification using the HaplotypeCaller tool. High quality variants were annotated
169 using snpEff (Cingolani et al., 2012) against the dog reference CanFam3.1.75.

170 The data were initially analyzed for known NCL genes. Given the apparent autosomal
171 recessive mode of transmission of the disease in the family, homozygous variants in
172 the coding exons or splicing regions of previously described NCL genes were
173 prioritized. Variants were identified in *CLN6*, *ARSG*, *TPP1* and *MFSD8* genes.
174 Segregation analysis for these candidates was performed by Sanger sequencing.
175 Following PCR amplification (see Table II for mutation location and primers used),
176 the PCR products were purified using ExoSAP-IT (USB), before direct Sanger
177 sequencing of both strands using BigDye Terminator v.3.1 chemistry v.3.1 (Applied
178 Biosystems) and an ABI 3730XL Genetic Analyzer (Applied Biosystems).
179 Sequencing traces were analyzed with Sequencher software v.4.2 (Gene Codes).

180

181 RESULTS

182 1. Clinical description of the patients

183 The affected Chihuahua dogs were a 1-year 10 month old male neutered and a 2-year
184 1 month old female at the time of presentation. The male started to demonstrate
185 clinical signs at 1 year 4 months of age and the female at one year of age. They both
186 demonstrated progressive vision deficits, pacing and behavioral changes. On
187 examination, the dogs appeared disorientated, poorly responsive and were bumping
188 into objects. They were ataxic on all limbs and had a wide-based stance. The female
189 dog also demonstrated an intermittent right head tilt. Proprioceptive positioning was
190 normal and there were mildly delayed hopping responses in all limbs. Segmental
191 spinal reflexes were normal. Menace responses were absent bilaterally with intact
192 dazzle reflexes and normal pupillary light reflexes. Remaining cranial nerves
193 examination, segmental spinal reflexes and vertebral column palpation were within
194 normal limits. No significant abnormalities were detected on physical examination,

195 including eye fundus examination. A complete blood count and biochemistry were
196 mainly unremarkable, with the exception of a moderate increase in liver enzymes and
197 bile acid stimulation tests in the male dog (Alanine aminotransferase: 372 IU/L –
198 reference interval (RI) <90; aspartate aminotransferase: 55 IU/L – RI<40; pre-
199 prandial bile acids: 5.3 $\mu\text{mol/L}$ – RI<5 and post prandial bile acids: 50 $\mu\text{mol/L}$ –
200 RI<15). MRI in both cases demonstrated a severe dilatation of the entire ventricular
201 system of the brain. The interthalamic adhesion appeared markedly decreased in size;
202 the cerebellar sulci and the fissures between the cerebellar folia were noticeably
203 widened. These changes suggested marked brain atrophy (Fig. 2A). Cerebrospinal
204 fluid (CSF) analysis was unremarkable. Urine organic acids were measured by mass
205 spectrometry in the male dog and were not suggestive of a disorder of organic acid
206 metabolism.

207 In light of the MRI changes, breed and in the absence of CSF abnormalities, a storage
208 disease, and more specifically NCL, was highly suspected. The dogs were discharged
209 with no treatment and the owners were warned of the very poor prognosis. Due to the
210 deterioration of the clinical signs, both owners elected for euthanasia of their dogs
211 within a month of discharge, but only the owners of the male dog agreed to post-
212 mortem examination.

213

214 2. Histopathological features

215 On gross examination of the brain, a moderate and symmetrical dilation of the lateral
216 ventricles was noted, associated with a thin cortex. Histopathological examination
217 demonstrated widespread amorphous to globular, eosinophilic to golden-brown,
218 intracytoplasmic storage material within neurons and astrocytes within the cerebral
219 cortex, basal ganglia, hippocampus, thalamus, brainstem and cerebellum (Fig. 2 and

220 3). All storage material within astrocytes and neurons stained variably magenta with
221 Periodic Acid-Schiff (PAS), variably positive with Sudan blue and intensively
222 positive with Luxol fast blue (Fig. 2C and D). When viewed under a microscope
223 equipped for epifluorescence illumination, as previously described (Katz et al.,
224 2005b), inclusion material fluoresced brightly (Fig. 2E). In the cortical grey matter
225 neuronal necrosis was absent but neuronal density was reduced and remnant laminar
226 neurons were disarrayed, and associated with an increased number of reactive
227 astrocytes and activated microglia. Within the cerebellum, Purkinje cells contained
228 abundant intracytoplasmic storage material. There was some disorganization and a
229 subjectively moderate decrease in the number of Purkinje cells, and several of the
230 remaining Purkinje cells showed a mildly shrunken with hypereosinophilic cytoplasm
231 and pyknotic nuclei (degeneration). Granular layer neurons were markedly reduced in
232 density (Fig. 3). Neurons within the pyramidal layer of the hippocampus contained
233 abundant intracytoplasmic storage but were present in normal numbers.

234 Immunohistochemical staining confirmed the marked neuroinflammation with a high
235 number of GFAP-positive astrocytes (Fig. 2G). Moreover, the tissue showed strong
236 staining against LAMP-1 (lysosomal-associated membrane protein 1), indicative of
237 alterations in this protein of the lysosome membrane (Fig. 2F). Finally, ganglion cells
238 within the retina were markedly reduced in number and when present contained
239 abundant intracytoplasmic storage material (Fig. 2I). Storage material was also found
240 in the duodenum, liver and heart using PAS staining and immunohistochemistry
241 against LAMP-1.

242 Based on these characteristics, NCL was diagnosed. NCL is a heterogeneous group of
243 diseases, and further characterization involves ultrastructural analysis of the storage

244 material. EM showed a complex multilamellar profile with presence of curvilinear
245 and rectilinear profiles (Fig. 2H).

246

247 3. Molecular analysis

248 Non synonymous mutations in the following previously known NCL genes were
249 identified: *ARSG* (p.Val262Asp), *CLN6* (p.Lys29Arg), *TPPI* (rs22973585) and
250 *MFSD8* (p.Phe282Leufs13*). *ARSG*, *CLN6* and *TPPI* variants did not segregate with
251 the disease phenotype and were therefore excluded as the causative mutations. The
252 *MFSD8* single pair deletion segregated within the available members of the family,
253 with affected dogs being homozygous for the mutation, both clinically unaffected
254 parents heterozygous for the mutation and clinically unaffected relatives either
255 heterozygous for the mutation or homozygous for the wild-type allele (Fig. 4). This
256 mutation is predicted to result in a severely truncated protein, which further supports
257 this to be the causal mutation.

258

259 DISCUSSION

260 In this study, we describe a family of dogs diagnosed with a mutation in *MFSD8*
261 (*CLN7*) resulting in neuronal ceroid lipofuscinosis. The mutation is predicted to
262 induce a frame shift leading to a premature stop codon.

263 The two littermates were monitored for clinical signs of degenerative brain disease,
264 mainly for the development of blindness, ataxia and cognitive impairment. These
265 changes, secondary to marked brain atrophy, are very similar to those observed in
266 patients affected with NCL or other animal forms of the disease. Presence of typical
267 autofluorescent cytoplasmic inclusions associated with marked neuronal loss and
268 astrocytosis confirmed the diagnosis of NCL. Numerous sporadic reports of

269 Chihuahua dogs affected with NCL have been described in the literature with a total
270 number of six previously described cases (Rac and Giesecke, 1975; Kuwamura et al.,
271 2003; Nakamoto et al., 2011). Similarities in age of onset, clinical signs and nature of
272 the inclusion make it likely that these animals were affected by the same mutation as
273 the dogs presented here. The previous descriptions concerned Chihuahua dogs from
274 Japan and Australia, which suggests a world-wide distribution of the mutation. It may
275 also be possible that the disease is not recognized by veterinarians, or that it is
276 confused with other diseases such as hydrocephalus that is relatively common in the
277 breed and can present with similar clinical signs. A commercial diagnostic test should
278 be considered in order to determine the frequency of the mutations and to eradicate it
279 from the breed.

280 Interestingly, the same mutation has recently been strongly suspected as the cause of
281 NCL in a single dog of another breed, the Chinese Crested, although lack of family
282 ancestry did not allow further confirmation by segregation analysis (Guo et al., 2015).
283 Our report is a further confirmation of this previously identified mutation. The clinical
284 signs, age of onset, imaging and pathologic findings were very similar to that
285 described here. The prevalence of the mutation in the Chinese crested population was
286 extremely low (only one heterozygous animal out of 1478 tested Chinese crested),
287 which makes it unlikely that a carrier animal could be found to start a colony to use as
288 animal model. The presence of the identical mutation in the two breeds would suggest
289 a common ancestor for the affected Chinese crested and Chihuahua dogs, possibly
290 through another dog breed from Mexico, the Mexican hairless dog (Xoloitzcuintle).
291 The Mexican hairless dogs and Chinese crested dogs are hairless dog breeds, which
292 are very likely to be related as they carry an identical mutation at the origin of their
293 alopecia (Drogemuller et al., 2008).

294

295 To identify the mutation, we sequenced the whole genome of one of the affected dogs
296 and compared it with the canine reference genome sequence. This allowed us to scan
297 initially for sequence variants in the coding and splicing regions of the canine
298 orthologs of the previously known genes to cause NCL in human patients. This
299 approach has been previously reported by others and was successful at finding
300 mutations causing NCL in dogs (Guo et al., 2014; Gilliam et al., 2015; Guo et al.,
301 2015). One of the genes (*ARSG*) considered as a candidate gene for NCL has now
302 been re-classified as causative of a form of mucopolysaccharidosis (MPS IIIE)
303 (Kowalewski et al., 2012; Kowalewski et al., 2015). However, the close proximity of
304 these neurodegenerative disorders made exclusion of a mutation in this gene
305 important.

306

307 In human patients, mutations in the *CLN7/MFSD8* gene generally result in a late-
308 infantile form, now called CLN7 disease. Symptoms are usually first noted between
309 the age of 2 to 7 years with seizures and developmental regression. Progression of the
310 disease results in motor and mental impairment, and blindness, leading to premature
311 death occurring before adulthood in most patients (Kousi et al., 2012). Despite being a
312 significant cause of late-infantile NCL in people (Aiello et al., 2009), very little is
313 known about the pathophysiology of CLN7, which is in part due to (until recently) the
314 lack of suitable animal models (Damme et al., 2014). MFSD8 is a lysosomal
315 membrane protein belonging to the major facilitator superfamily (MFS). It is thought
316 to act as a transporter but its substrate is still currently unknown (Damme et al., 2014).
317 A mouse model of *Mfsd8* disruption has been created and should contribute to a better
318 understanding of this form of NCL, especially regarding the function of the protein

319 and the disease mechanisms. Unfortunately, this model has limitations, as it does not
320 accurately reproduce the clinical and histopathological findings seen in human
321 patients (Damme et al., 2014). No obvious neuronal loss is observed in these mice,
322 although marked accumulation of autofluorescent material in the nerve cells and
323 retinal degeneration (photoreceptor layer) is evident. The failure to reproduce all key-
324 features of the human disease may be due to the presence of residual Cln7 protein
325 function in these mice. In contrast, the Chihuahua dogs presented here could represent
326 a better model as the histopathologic findings mimic the human pathology with
327 marked neuronal loss and astrogliosis, resulting in progression of neurological signs
328 incompatible with life (Table III). In the dog presented here, the Purkinje cells layer
329 appears relatively spared - although signs of degeneration are visible – compared to
330 what is observed in human patients. This difference could be due to the fact that the
331 dog has been euthanized at a reasonably early stage of the disease. Indeed, this layer
332 tends to be progressively lost in patients contrary to the granular cells layer, which is
333 completely lost at very early age (Elleder et al., 2011). Overall, canine models are a
334 good complement to murine models, especially for assessment of potential therapies
335 due to a closer phenotype and longer lifespan (Faller et al., 2015). Additionally, the
336 Chihuahua breed would be a particularly promising model due to its reasonably small
337 size and ease of handling, which would make them particularly suitable as research
338 individuals. However, further histological characterization of dogs of both sexes and
339 of different ages would be needed for a better understanding of the progression of the
340 disease.

341

342 In conclusion, we have identified a mutation in *MFSD8* causing Neuronal Ceroid
343 Lipofuscinosis in Chihuahua dogs. This breed could represent a good animal model of
344 CLN7 disease.

345

346 CONFLICT OF INTEREST STATEMENT

347 The authors have no conflict of interest to declare.

348

349 ROLES OF AUTHORS

350 All authors had full access to the data in the study and take responsibility for the
351 integrity of the data and the accuracy of the data analysis.

352 KF examined one of the affected dogs, genotyped and sequenced samples from some
353 variants and drafted the manuscript. JB conceived the mutation identification strategy,
354 identified the variants in the sequence alignment and drafted the manuscript. SS
355 performed the post-mortem and histopathological examinations and interpreted the
356 pathologic findings. GWA performed advanced histological analysis. LD and CKR
357 genotyped and sequenced samples from some variants. JA interpreted electron
358 microscopy findings. JP supervised the clinical diagnosis and secured funding. SEM
359 provided input on NCL disease. RGQ examined one of the affected dogs, supervised
360 the clinical diagnosis, secured funding and drafted the manuscript. RJG conceived the
361 mutation identification strategy, supervised PCR amplification and Sanger sequencing
362 and drafted the manuscript. All authors read, revised critically and approved the final
363 manuscript.

364

365 ACKNOWLEDGEMENTS

366 We would like to thank Ms Jennifer Barrie for her help in the preparation of the
367 electron microscopy samples, Dr Francesco Marchesi for the histological
368 photographs and Drs Mark McLaughlin and Intan Shafie for their help with DNA
369 extraction. We are also grateful to the breeder and the owners of the affected dogs and
370 of controls dogs for providing us with the samples.

371

372

373 LITTERATURE CITED

- 374 Abitbol M, Thibaud JL, Olby NJ, Hitte C, Puech JP, Maurer M, Pilot-Storck F, Hedan
375 B, Dreano S, Brahimi S, Delattre D, Andre C, Gray F, Delisle F, Caillaud C,
376 Bernex F, Panthier JJ, Aubin-Houzelstein G, Blot S, Tiret L. 2010. A canine
377 Arylsulfatase G (ARSG) mutation leading to a sulfatase deficiency is
378 associated with neuronal ceroid lipofuscinosis. *Proceedings of the*
379 *National Academy of Sciences of the United States of America*
380 *107(33):14775-14780.*
- 381 Aiello C, Terracciano A, Simonati A, Discepoli G, Cannelli N, Claps D, Crow YJ,
382 Bianchi M, Kitzmuller C, Longo D, Tavoni A, Franzoni E, Tessa A, Veneselli
383 E, Boldrini R, Filocamo M, Williams RE, Bertini ES, Biancheri R, Carrozzo
384 R, Mole SE, Santorelli FM. 2009. Mutations in MFSD8/CLN7 are a frequent
385 cause of variant-late infantile neuronal ceroid lipofuscinosis. *Human*
386 *mutation* *30(3):E530-540.*
- 387 Anderson GW, Goebel HH, Simonati A. 2013. Human pathology in NCL.
388 *Biochimica et biophysica acta* *1832(11):1807-1826.*
- 389 Awano T, Katz ML, O'Brien DP, Taylor JF, Evans J, Khan S, Sohar I, Lobel P,
390 Johnson GS. 2006. A mutation in the cathepsin D gene (CTSD) in American
391 Bulldogs with neuronal ceroid lipofuscinosis. *Molecular genetics and*
392 *metabolism* *87(4):341-348.*
- 393 Cingolani P, Platts A, Wang le L, Coon M, Nguyen T, Wang L, Land SJ, Lu X, Ruden
394 DM. 2012. A program for annotating and predicting the effects of single
395 nucleotide polymorphisms, SnpEff: SNPs in the genome of *Drosophila*
396 *melanogaster* strain w1118; iso-2; iso-3. *Fly* *6(2):80-92.*
- 397 Damme M, Brandenstein L, Fehr S, Jankowiak W, Bartsch U, Schweizer M,
398 Hermans-Borgmeyer I, Storch S. 2014. Gene disruption of Mfsd8 in mice
399 provides the first animal model for CLN7 disease. *Neurobiology of disease*
400 *65:12-24.*
- 401 DePristo MA, Banks E, Poplin R, Garimella KV, Maguire JR, Hartl C, Philippakis
402 AA, del Angel G, Rivas MA, Hanna M, McKenna A, Fennell TJ, Kernysky
403 AM, Sivachenko AY, Cibulskis K, Gabriel SB, Altshuler D, Daly MJ. 2011. A
404 framework for variation discovery and genotyping using next-generation
405 DNA sequencing data. *Nature genetics* *43(5):491-498.*
- 406 Di Fruscio G, Schulz A, De Cegli R, Savarese M, Mutarelli M, Parenti G, Banfi S,
407 Braulke T, Nigro V, Ballabio A. 2015. Lysoplex: An efficient toolkit to
408 detect DNA sequence variations in the autophagy-lysosomal pathway.
409 *Autophagy* *11(6):928-938.*
- 410 Drogemuller C, Karlsson EK, Hytonen MK, Perloski M, Dolf G, Sainio K, Lohi H,
411 Lindblad-Toh K, Leeb T. 2008. A mutation in hairless dogs implicates
412 FOXI3 in ectodermal development. *Science* *321(5895):1462.*
- 413 Elleder M, Kousi M, Lehesjoki AE, Mole SE, Siintola E, Topcu M. 2011. CLN7. In:
414 Mole SE, Williams RE, Goebel HH, editors. *The neuronal ceroid*
415 *lipofuscinoses (Batten disease)*. 2nd ed. Oxford: Oxford University Press.
- 416 Faller KM, Gutierrez-Quintana R, Mohammed A, Rahim AA, Tuxworth RI, Wager
417 K, Bond M. 2015. The neuronal ceroid lipofuscinoses: Opportunities from
418 model systems. *Biochimica et biophysica acta* *1852(10 Pt B):2267-2278*
- 419 Farias FH, Zeng R, Johnson GS, Wininger FA, Taylor JF, Schnabel RD, McKay SD,
420 Sanders DN, Lohi H, Seppala EH, Wade CM, Lindblad-Toh K, O'Brien DP,

421 Katz ML. 2011. A truncating mutation in ATP13A2 is responsible for
422 adult-onset neuronal ceroid lipofuscinosis in Tibetan terriers.
423 *Neurobiology of disease* 42(3):468-474.

424 Gilliam D, Kolicheski A, Johnson GS, Mhlanga-Mutangadura T, Taylor JF, Schnabel
425 RD, Katz ML. 2015. Golden Retriever dogs with neuronal ceroid
426 lipofuscinosis have a two-base-pair deletion and frameshift in CLN5.
427 *Molecular genetics and metabolism* 115(2-3):101-109.

428 Guo J, Johnson GS, Brown HA, Provencher ML, da Costa RC, Mhlanga-
429 Mutangadura T, Taylor JF, Schnabel RD, O'Brien DP, Katz ML. 2014. A
430 CLN8 nonsense mutation in the whole genome sequence of a mixed breed
431 dog with neuronal ceroid lipofuscinosis and Australian Shepherd
432 ancestry. *Molecular genetics and metabolism* 112(4):302-309.

433 Guo J, O'Brien DP, Mhlanga-Mutangadura T, Olby NJ, Taylor JF, Schnabel RD, Katz
434 ML, Johnson GS. 2015. A rare homozygous MFSD8 single-base-pair
435 deletion and frameshift in the whole genome sequence of a Chinese
436 Crested dog with neuronal ceroid lipofuscinosis. *BMC veterinary research*
437 10:960.

438 Jolly RD, Palmer DN. 1995. The neuronal ceroid-lipofuscinoses (Batten disease):
439 comparative aspects. *Neuropathol Appl Neurobiol* 21(1):50-60.

440 Katz ML, Farias FH, Sanders DN, Zeng R, Khan S, Johnson GS, O'Brien DP. 2011. A
441 missense mutation in canine CLN6 in an Australian shepherd with
442 neuronal ceroid lipofuscinosis. *J Biomed Biotechnol* 2011:198042.

443 Katz ML, Khan S, Awano T, Shahid SA, Siakotos AN, Johnson GS. 2005a. A
444 mutation in the CLN8 gene in English Setter dogs with neuronal ceroid-
445 lipofuscinosis. *Biochem Biophys Res Commun* 327(2):541-547.

446 Katz ML, Narfstrom K, Johnson GS, O'Brien DP. 2005b. Assessment of retinal
447 function and characterization of lysosomal storage body accumulation in
448 the retinas and brains of Tibetan Terriers with ceroid-lipofuscinosis. *Am J*
449 *Vet Res* 66(1):67-76.

450 Kousi M, Lehesjoki AE, Mole SE. 2012. Update of the mutation spectrum and
451 clinical correlations of over 360 mutations in eight genes that underlie the
452 neuronal ceroid lipofuscinoses. *Human mutation* 33(1):42-63.

453 Kowalewski B, Heimann P, Ortkras T, Lullmann-Rauch R, Sawada T, Walkley SU,
454 Dierks T, Damme M. 2015. Ataxia is the major neuropathological finding
455 in arylsulfatase G-deficient mice: similarities and dissimilarities to
456 Sanfilippo disease (mucopolysaccharidosis type III). *Human molecular*
457 *genetics* 24(7):1856-1868.

458 Kowalewski B, Lamanna WC, Lawrence R, Damme M, Stroobants S, Padva M,
459 Kalus I, Frese MA, Lubke T, Lullmann-Rauch R, D'Hooge R, Esko JD, Dierks
460 T. 2012. Arylsulfatase G inactivation causes loss of heparan sulfate 3-O-
461 sulfatase activity and mucopolysaccharidosis in mice. *Proceedings of the*
462 *National Academy of Sciences of the United States of America*
463 109(26):10310-10315.

464 Kuwamura M, Hattori R, Yamate J, Kotani T, Sasai K. 2003. Neuronal ceroid-
465 lipofuscinosis and hydrocephalus in a chihuahua. *J Small Anim Pract*
466 44(5):227-230.

467 Li H, Durbin R. 2009. Fast and accurate short read alignment with Burrows-
468 Wheeler transform. *Bioinformatics* 25(14):1754-1760.

469 McKenna A, Hanna M, Banks E, Sivachenko A, Cibulskis K, Kernytsky A, Garimella
470 K, Altshuler D, Gabriel S, Daly M, DePristo MA. 2010. The Genome Analysis
471 Toolkit: a MapReduce framework for analyzing next-generation DNA
472 sequencing data. *Genome research* 20(9):1297-1303.

473 Melville SA, Wilson CL, Chiang CS, Studdert VP, Lingaas F, Wilton AN. 2005. A
474 mutation in canine CLN5 causes neuronal ceroid lipofuscinosis in Border
475 collie dogs. *Genomics* 86(3):287-294.

476 Mole SE, Williams RE. 2001 [Updated 2013]. Neuronal Ceroid-Lipofuscinoses. In:
477 Pagon RA, Adam MP, Ardinger HH, Wallace SE, Amemiya A, Bean LJH, Bird
478 TD, Dolan CR, Fong CT, Smith RJH, Stephens K, editors. *GeneReviews(R)*
479 [Internet]. Seattle (WA): University of Washington, Seattle. Available
480 from: <http://www.ncbi.nlm.nih.gov/books/NBK1428/>.

481 Nakamoto Y, Yamato O, Uchida K, Nibe K, Tamura S, Ozawa T, Ueoka N, Nukaya A,
482 Yabuki A, Nakaichi M. 2011. Neuronal ceroid-lipofuscinosis in longhaired
483 Chihuahuas: clinical, pathologic, and MRI findings. *J Am Anim Hosp Assoc*
484 47(4):e64-70.

485 Rac R, Giesecke PR. 1975. Letter: Lysosomal storage disease in chihuahuas.
486 *Australian veterinary journal* 51(8):403-404.

487 Sanders DN, Farias FH, Johnson GS, Chiang V, Cook JR, O'Brien DP, Hofmann SL,
488 Lu JY, Katz ML. 2010. A mutation in canine PPT1 causes early onset
489 neuronal ceroid lipofuscinosis in a Dachshund. *Molecular genetics and*
490 *metabolism* 100(4):349-356.

491 Shacka JJ. 2012. Mouse models of neuronal ceroid lipofuscinoses: useful pre-
492 clinical tools to delineate disease pathophysiology and validate
493 therapeutics. *Brain Res Bull* 88(1):43-57.

494 Wohlke A, Philipp U, Bock P, Beineke A, Lichtner P, Meitinger T, Distl O. 2011. A
495 one base pair deletion in the canine ATP13A2 gene causes exon skipping
496 and late-onset neuronal ceroid lipofuscinosis in the Tibetan terrier. *PLoS*
497 *Genet* 7(10):e1002304.

498

499

500 FIGURE LEGENDS

501

502 Figure 1: Pedigree of the family of Chihuahua dogs. Solid figures represent affected
503 dogs, whereas plain figures are clinically unaffected dogs. Squares represent males
504 and circles females. Genotypes of the tested dogs are mentioned under each figure
505 with WT = wild-type allele and Del = *MFSD8*:c.843delT;p.Phe282Leufs13* allele.

506

507 Figure 2: Magnetic resonance imaging and histological findings of the male dog. A:
508 Sagittal T2-weighted image of the brain. Note the marked generalised cerebral
509 atrophy. B: H&E staining of the cerebellum at high magnification showing inclusions
510 within the Purkinje cells (arrows). C & D: Periodic acid-Schiff (C) and Luxol Fast
511 Blue (D) staining of brainstem neurons at high magnification. E: Fluorescence cryostat
512 section of the cerebral cortex showing abundant autofluorescent inclusions. F & G:
513 Lysosomal staining by use of anti-LAMP-1 antibody of the cerebellum of the affected
514 dog (F) and of a control dog (G). H: Immunostaining against GFAP (brainstem). I:
515 Electron microscopy of the storage bodies from the cerebral cortex. Note the mixed
516 nature of the inclusions with curvilinear (*) and rectilinear (arrow) profiles. J. H&E
517 staining of a retinal section. Note the marked depletion of the ganglion cells.
518 NFL: nerve fiber layer. GCL: ganglion cell layer. IPL: inner plexiform layer. INL:
519 inner nuclear layer. OPL: outer plexiform layer. ONL: outer nuclear layer. RL:
520 receptor layer.

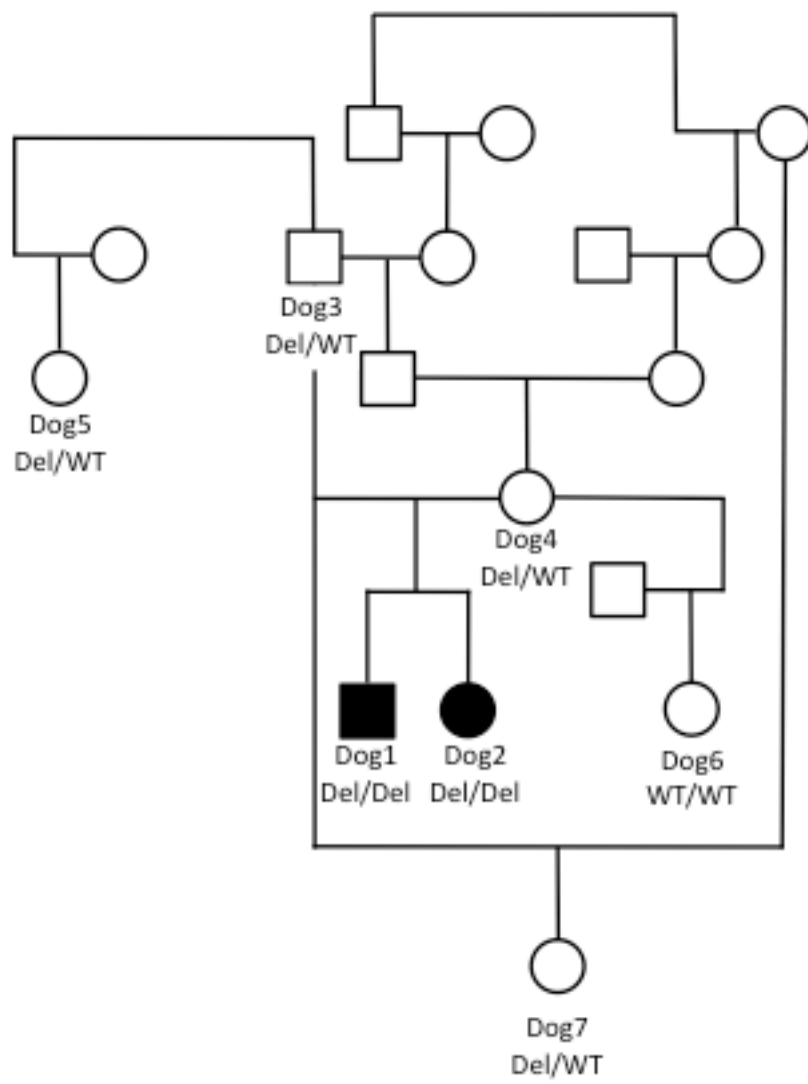
521

522 Figure 3: H&E sections of the vermis of the cerebellum of the affected dog (A1 and
523 A2) and of a control dog (B1 and B2) at low and high magnification. Note the marked
524 depletion in granule cells in the affected dog (the blue line in each panel spans the

525 granular layer). This results in an overall marked atrophy of the cerebellar cortex. In
526 the affected dog, there is a moderate decrease in number of Purkinje cells (*), which
527 show signs of degeneration. NB: in the control dog, at high magnification (B2), the
528 white lamina is not seen due to the normal thickness of the granule cell layer,
529 preventing visualisation of the white lamina in the same image as the three layers of
530 cerebellar grey matter.

531

532 Figure 4: Sequence traces showing a small portion of the genomic DNA of the
533 Chihuahua dogs shown in the pedigree (Fig. 2), and centered around the mutation of
534 interest (*MFSD8*:c.843delT:p.Phe282Leufs13*). All sequences are aligned against the
535 canine reference genome (CanFam3.1).



536
537
538

Figure 1

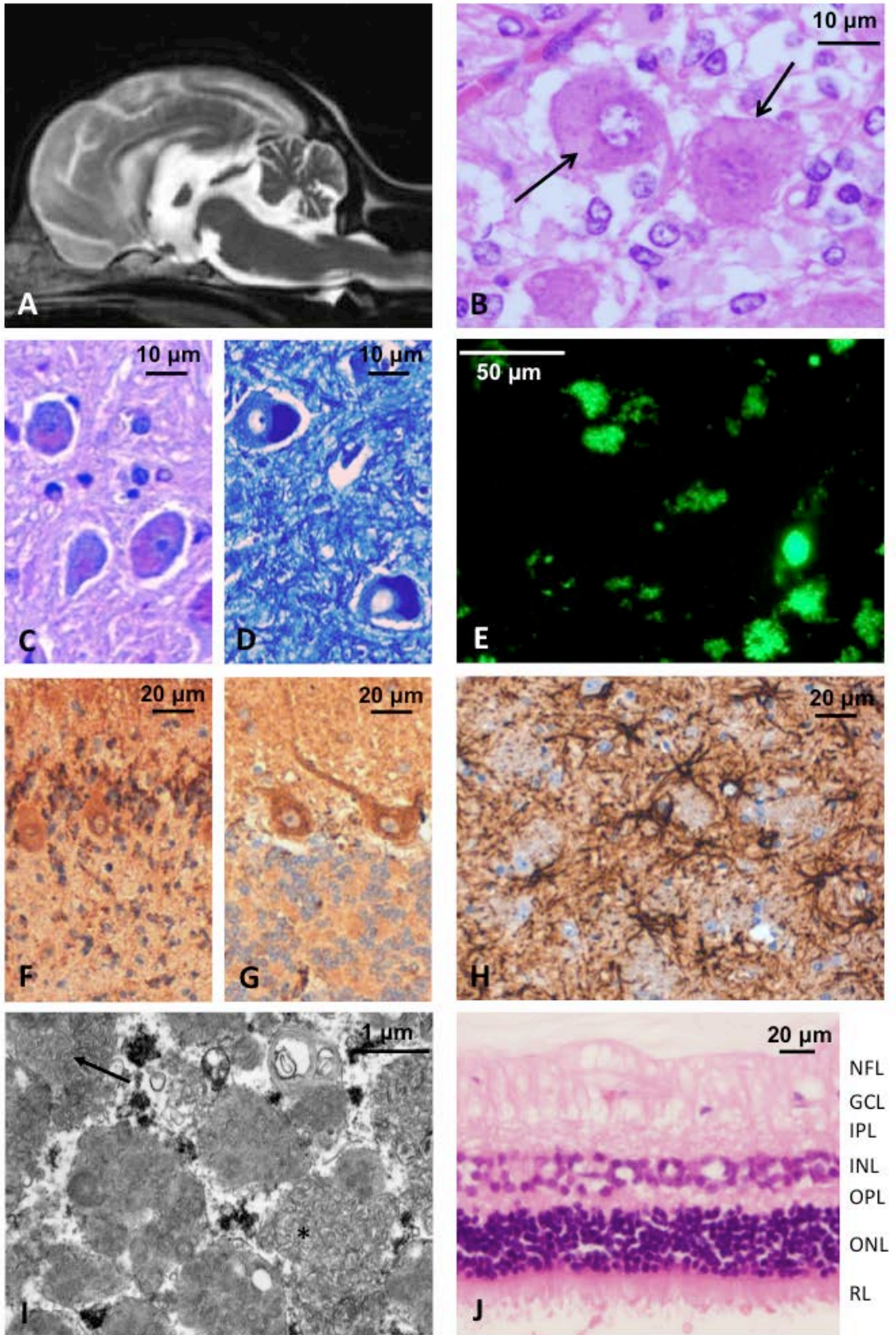


Figure 2

539
 540
 541

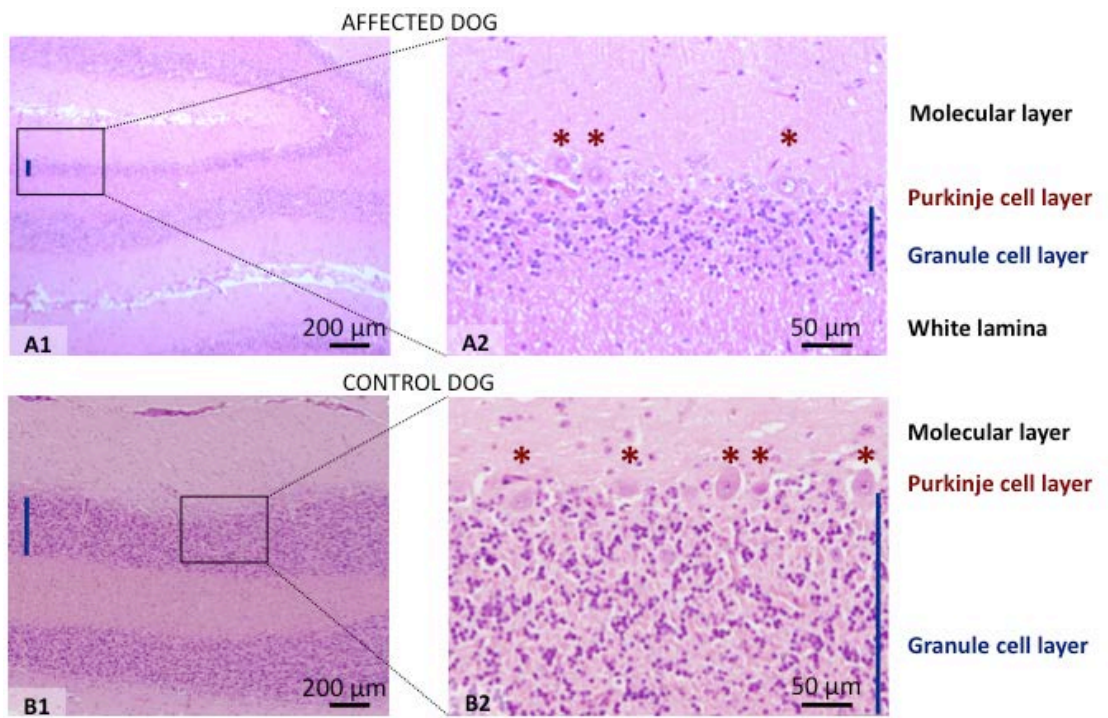


Figure 3

542
543

Reference **AATATTGTGTTTTTCGTGATTCATTTATCTTTGCCCTTTTTGAAACGTAAGTT**
 Dog1 **AATATTGTGTTTTTCGTGATTCATT : ATCTTTGCCCTTTTTGAAACGTAAGTT**
 Dog2 **AATATTGTGTTTTTCGTGATTCATT : ATCTTTGCCCTTTTTGAAACGTAAGTT**
 Dog3 **AATATTGTGTTTTTCGTGATTCATT : ATCTTTGGCCCTTTGAAACGTAAGTT**
 Dog4 **AATATTGTGTTTTTCGTGATTCATT : ATCTTTGGCCCTTTGAAACGTAAGTT**
 Dog5 **AATATTGTGTTTTTCGTGATTCATT : ATCTTTGGCCCTTTGAAACGTAAGTT**
 Dog6 **AATATTGTGTTTTTCGTGATTCATTTATCTTTGCCCTTTTTGAAACGTAAGTT**
 Dog7 **AATATTGTGTTTTTCGTGATTCATT : ATCTTTGGCCCTTTGAAACGTAAGTT**

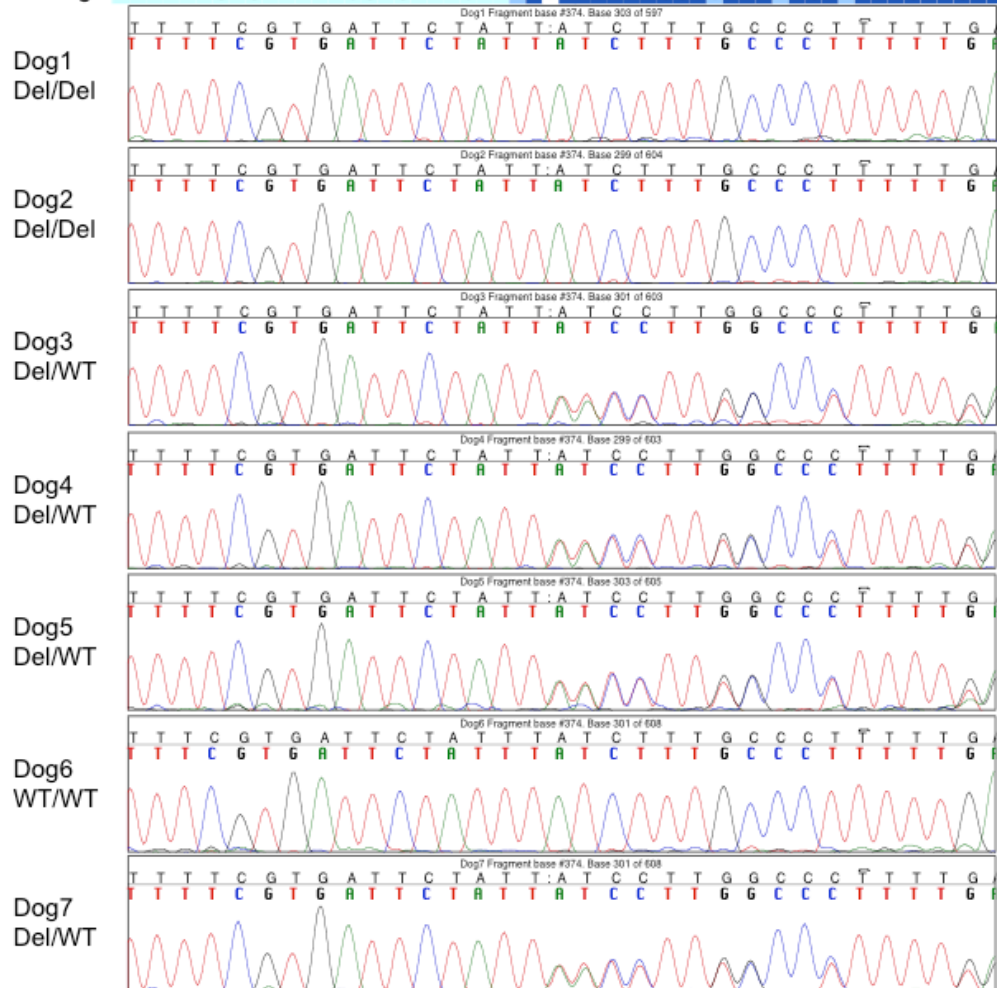


Figure 4

544
 545
 546

547 *Table I. Table of Primary Antibodies Used.*

548

Antigen	Description of Immunogen	Source, Host Species, Cat. #, Clone or Lot#, RRID	Concentration Used
LAMP-1	Lysosomal associated membrane protein 1	Abcam, mouse monoclonal, Cat# ab25630 RRID : AB_470708	1:200
Glial fibrillary acidic protein (GFAP)	GFAP isolated from bovine spinal cord	Dako, Rabbit monoclonal, Cat# Z0334, RRID:AB_2314535	1:1000

549

550

551 *Table II: Homozygous variants in the coding region or splicing areas of previously*
 552 *known NCL genes used for Sanger sequencing confirmation and segregation*
 553 *analyses.*

Gene (transcript)	Variant location	Primers
ARSG (XM_005624176.1)	p.Val262Asp	F: 5'-ACCTCTTGGCTTTCCCATTG-3' R: 5'-CAGGGAGCTAGCTGGGTTTT-3'
CLN6 (NM_001011888.1)	p.Lys29Arg	F: 5'-CACAGTGCTTCCCGCAAC-3' R: 5'-CACCAAACCGCATCCTACT-3'
TPP1 (NM_001013847.1)	Splice site (rs22973585)	F: 5'-GCTCACAGTGTGCACATGTG-3' R: 5'-GAGTACCTGATGAGTGCCGG-3'
CLN7/MFSD8 (XM_533294.4)	c.843delT; p.F282Lfs13*	F: 5'-ATCTCCTGGGAAGAAAATTCAC-3' R: 5'-TTAAATCATGGCACTGAAGTTTT-3'

554
 555 *Only the mutation identified in MFSD8:c.843delT:p.Phe282Leufs13* segregated with*
 556 *the disease in the studied family.*

557
 558
 559

560 *Table III: Comparison of the phenotypes of human CLN7 disease, the $Mfsd8^{(tm1a/tm1a)}$*
561 *mouse model (Damme et al., 2014) and the canine model described here and in the*
562 *literature.*

Neuropathological features	CLN7 disease (humans)	$Mfsd8^{(tm1a/tm1a)}$ (mice) (Damme et al 2014)	CLN7 disease (canine)
Retinal degeneration	Yes	Yes	Yes (this report, Kuwamura <i>et al.</i> , 2003)
Accumulation of SCMAS (Sub-unit C of mitochondrial ATP synthase)	Yes	Yes	Not performed
Accumulation of autofluorescent ceroid lipopigments	Yes	Yes	Yes (this report; Kuwamura <i>et al.</i> , 2003; Guo <i>et al.</i> , 2015)
Astrogliosis	Yes	Only mildly	Yes (this report, Guo <i>et al.</i> , 2015; Kuwamura <i>et al.</i> , 2003; Nakamoto <i>et al.</i> , 2011)
Generalised seizures	Yes	No	No (this report; Guo <i>et al.</i> , 2015; Kuwamura <i>et al.</i> , 2003) Suspected partial seizure (jaw chomping) (Rac <i>et al.</i> , 1975) Terminal stage (Nakamoto <i>et al.</i> , 2011)
Myoclonus/ataxia	Yes	Yes	Yes (ataxia) (this report; Guo <i>et al.</i> , 2015; Rac <i>et al.</i> , 1975; Nakamoto <i>et al.</i> , 2011)
Neuronal loss / brain atrophy	Yes	No	Yes (this report, Guo <i>et al.</i> , 2015; Rac <i>et al.</i> , 1975; Nakamoto <i>et al.</i> , 2011; Kuwamura <i>et al.</i> , 2003)
Premature death	Yes (mean age 11.5 years) (Kousi et al	No	Yes (euthanasia as not compatible with life) –

2009)

~ 1.5 - 2 years (lifespan
of a Chihuahua or a
Chinese Crested dog >
12 years) (this report;
Kuwamura *et al.*, 2003;
Rac *et al.*, 1975;
Nakamoto *et al.*, 2011;
Guo *et al.*, 2015).

563 *Table adapted from Damme et al. (2014)*